

Transforming characteristics of the Rogowski coil current transformer with a digital integrator for high-frequency signals

eISSN 2051-3305

Received on 30th August 2018

Revised 12th November 2018

Accepted on 12th November 2018

E-First on 6th February 2019

doi: 10.1049/joe.2018.8850

www.ietdl.org

Fubin Pang¹ ✉, Yu Liu¹, Jianfei Ji¹, Chi Zhang¹¹Relay and Protection Department, State Grid Jiangsu Electric Power Co. Ltd. Research Institute, Nanjing, People's Republic of China

✉ E-mail: pangfubin2006@163.com

Abstract: The Rogowski coil current transformer is widely used in intelligent substations for its rapid response, wide bandwidth measurement, and non-magnetic saturation. In most cases, it works with a digital integrator to restore the differential signal output by the coil. However, its output waveform can be deformed when transforming high-frequency signals generated in the transient process of the power system. The working process of the Rogowski coil current transformer is presented, including Rogowski coil head transferring, analogue filter filtering, analogue-to-digital converter sampling, and digital integrator restoring. The reason for the waveform deformation when transforming high-frequency signals is investigated by theoretical derivation. In order to show the waveform deformation phenomenon, an experiment is devised and the results output by the Rogowski coil transformer and low power current transformer are compared and analysed. Several measures to improve the output waveform deformation are proposed, such as increasing the sampling rate of the converter, decreasing the cut-off frequency of the filter, or replacing the digital integrator with the analogue integrator. The researches provide important guidelines for the application of the Rogowski coil current transformer with the digital integrator in the case of frequency aliasing.

1 Introduction

In recent years, the Rogowski coil current transformer is widely used for measuring very wide range currents from a few milliamperes to thousands of kiloamperes without saturating because of its non-magnetic core, with the bandwidth reaching up to a few megahertz that enable the transformer to measure the rapidly changing current waveforms [1, 2]. Due to the differential output voltage generated by the input current, it usually works with an integrator to restore the current. Generally, there are two kinds of integrators: one is analogue integrator and the other is digital integrator [3]. Compared with the analogue integrator which is usually influenced by the temperature and some other environmental factors, the digital integrator is usually adopted for its higher stability and more accurate transforming performance in current measurement [4, 5].

However, it has been found that the current measuring system usually fails in the measurement of high-frequency signals, and the output of the Rogowski coil current transformer is greatly distorted due to the frequency aliasing in the sampling link. Since the digital integrator cannot response the waveform in the high-frequency spectrum, the measured waveform on the tail part deviates from the original input wave. In this paper, the working process of the Rogowski coil current transformer is presented, including the differential operation, data sampling, and integrating links. To show the frequency aliasing phenomenon vividly, the results output by the Rogowski coil current transformer using the digital integrator and the low power current transformer (LPCT) are compared, and the improving methods to restore the measured high-frequency signals are proposed, such as increasing the sampling rate of the converter, decreasing the cut-off frequency of the filter, or adopting the analogue integrator rather than the digital integrator. Advantages and disadvantages of each method are compared to provide a more comprehensive review of the effective measures. The research in this paper is of great significance for the application of the Rogowski coil current transformer.

2 Principle

2.1 Rogowski coil measuring principle

The Rogowski coil works by sensing the magnetic field in the space around the conductor. Ampere's law provides the relationship between the current flowing through the conductor and the magnetic field around it [6, 7]. The Rogowski coil is composed of the enameled wire even winding on the ceramic or other non-ferromagnetic frame whose differential permeability is close to that of the air [8]. If a single-turn coil is placed perpendicular to this magnetic field so that the flux lines can link the coil, a voltage will be generated according to Faraday's law [9].

Fig. 1 illustrates the measuring principle of the Rogowski coil. According to the Ampere circuit rule, the equations of magnetic flux can be obtained as follows [10, 11]:

$$\begin{cases} \oint_l H dl = I \\ B = \mu_0 H \\ \psi = N \int_S B dS \end{cases} \quad (1)$$

where H and B are the magnetic field intensity and density at the defined point, respectively, and ψ is the sum of the magnetic flux of the coil. For the point away from the centre of the coil, the magnetic field density is

$$B = \mu_0 H = \frac{\mu_0 I}{2\pi r} \quad (2)$$

The induction electromotive force generated from the coil would be [12]

$$e = - \frac{d\psi}{dt} \quad (3)$$

2.2 Input and output relationship of the Rogowski coil

In most cases, the termination resistance is a determining factor of the Rogowski coil, and the equivalent circuit diagram of the

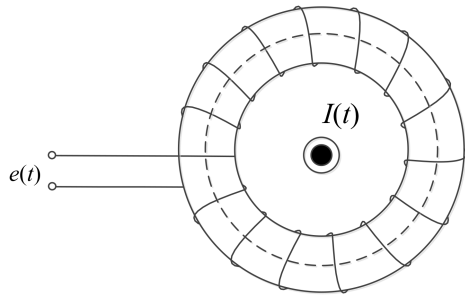


Fig. 1 Measuring principle of a Rogowski coil

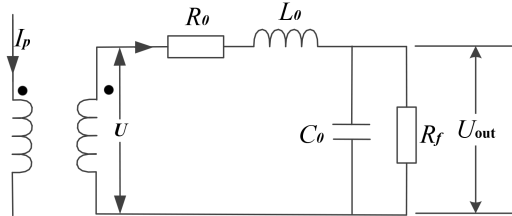


Fig. 2 Equivalent circuit of a Rogowski coil

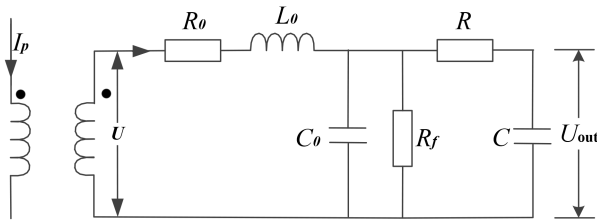


Fig. 3 Typical circuit diagram of an external-integrating Rogowski coil

lumped parameter model is shown in Fig. 2. In this figure, R_0 is the coil self-resistance, L_0 is the coil self-inductance, C_0 is the coil self-capacitance, and R_f is the coil termination resistance. According to the measuring principle of the Rogowski coil, the relationship between the input and output of the coil can be obtained as

$$U = -M \frac{dI_p}{dt} \quad (4)$$

As shown in Fig. 2, the output voltage between the termination resistance and that of the coil can be deduced from the following equation:

$$\frac{U}{U_{out}} = \frac{R_0 + j\omega L_0 + [(R_f/j\omega C_0)/((1/j\omega C_0) + R_f)]}{[(R_f/j\omega C_0)/((1/j\omega C_0) + R_f)]} \quad (5)$$

By introducing $s = j\omega$, the relationship between the output voltage of the termination resistance and primary current can be expressed as follows:

$$H(s) = \frac{U_{out}}{I_p} = \frac{MR_f s}{R_f C_0 L_0 s^2 + (R_f C_0 R_0 + L_0)s + (R_0 + R_f)} \quad (6)$$

In order to simplify the analysis, the self-capacitance C_0 can be ignored and (6) can be written as follows:

$$H(s) = \frac{MR_f s}{L_0 s + (R_0 + R_f)} = \frac{MR_f}{L_0} \frac{Ts}{Ts + 1} \quad (7)$$

where $T = L_0/(R_0 + R_f)$. Assume that $\omega_0 = 1/T$; obviously, ω_0 is the terminating frequency of the Rogowski coil, and its magnitude and phase of the transfer function can further be obtained, respectively, as

$$\begin{cases} \text{mag}(\omega) = \frac{MR_f}{L_0} \left| \frac{j\omega}{j\omega + \omega_0} \right| = \frac{MR_f}{L_0} \frac{\omega}{\sqrt{\omega^2 + \omega_0^2}} \\ \text{phase}(\omega) = 90^\circ - \arctan \frac{\omega}{\omega_0} \end{cases} \quad (8)$$

2.3 Self-integrating and external integrating

From (8), it can be seen that when $\omega \gg \omega_0$ ($\omega L_0 \gg R_0 + R_f$), the magnitude gain of the Rogowski coil is MR_f/L_0 and the phase transfer is close to 0° . The coil is called the self-integrating Rogowski coil, and it is suitable to measure short duration pulsed current [13, 14].

Suppose that $\omega \ll \omega_0$ ($\omega L_0 \ll R_0 + R_f$); then the transfer relationship in (8) can be written as $H(s) = Ms$. In that case, the primary current could be reconstructed when there is an integrator in the end of the Rogowski coil. The coil is called the external-integrating Rogowski coil, and it is suitable to measure a long-duration pulsed current. The typical circuit diagram of the external-integrating Rogowski coil is shown in Fig. 3.

From Fig. 3, the relationship between the output voltage of the integrator and the input primary current can be expressed as follows:

$$\begin{aligned} H(s) &= \frac{U_{out}}{I_p} \\ &= \frac{Ms}{C_0 L_0 s^2 + (C_0 R_0 + (L_0/R_f)s + ((R_0/R_f) + 1)RCs + 1} \end{aligned} \quad (9)$$

When the self-capacitance C_0 is ignored, the transfer function of the Rogowski coil becomes

$$H(s) = \frac{U_{out}}{I_p} = \frac{Ms}{(L_0/R_f)s + ((R_0/R_f) + 1)RCs + 1} \quad (10)$$

2.4 Analogue and digital integrators

Generally, there are two kinds of integrators, namely the analogue integrator and the digital integrator. The working process of each integrator is shown in Figs. 4 and 5. It can be seen that the difference between the two is that when using the analogue integrator, the integrating link is ahead of the waveform filtering, while when using the digital integrator, it is after the analogue-to-digital (A/D) sampling. In the frontier working process, the input primary current is implemented differential operation when it passes the Rogowski coil, and the signal is immediately restored in the integrating link; then it is filtered and converted into the digital signal after the A/D sampling. The primary current is restored without waveform deformation. However, in the digital integrator working process, the frequency aliasing occurs in the case of high-frequency input because the integrating link to restore the signal is after the sampling link. Assume that the input signal frequency is f_0 , the initial phase is φ_0 , and the magnitude is A ; then the expression of the input can be expressed as follows:

$$y(t) = A \sin(2\pi f_0 t + \varphi_0) \quad (11)$$

When the transformation ratio is $A:1$, the magnitude gain and the phase transfer are m and $\pi/2$, respectively, due to the differential operation, and the output of the Rogowski coil is written as follows:

$$y(t) = m \sin\left(2\pi f_0 t + \frac{\pi}{2} + \varphi_0\right) \quad (12)$$

Before the signal is sampled, it must pass through the filter. Assume that the magnitude gain and phase transfer is A_f and φ_f , respectively. The output of the filter is obtained as follows:

$$y_f(t) = mA_f \sin\left(2\pi f_0 t + \frac{\pi}{2} + \varphi_0 + \varphi_f\right) \quad (13)$$

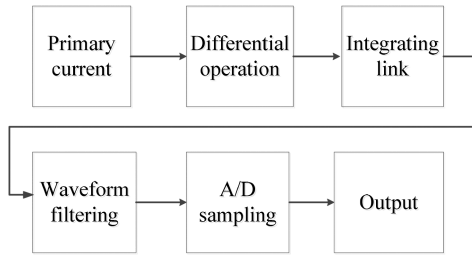


Fig. 4 Working process of the Rogowski coil using an analogue integrator

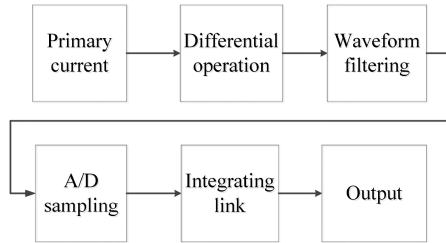


Fig. 5 Working process of the Rogowski coil using a digital integrator

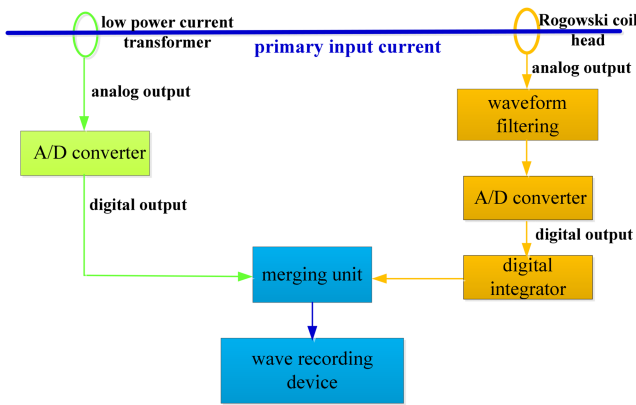


Fig. 6 Principle of the experiment

Table 1 Input signal types

No.	Frequency, Hz	Value, A	Initial phase (°)
1	50	100	0
2	3950	100	0
3	4000	100	0

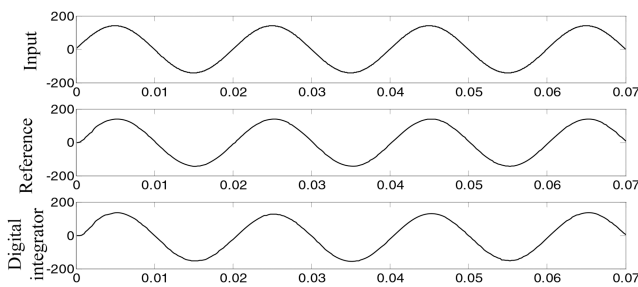


Fig. 7 Results of the 50 Hz input signal

For the analogue integrator, assume that the sampling frequency of the A/D converter is f_s and

$$f_0 = \beta f_s \quad (14)$$

where β is a positive factor, and then the output of the sampling converter is

$$\begin{aligned} y_f[n] &= mA_f \sin\left(2\pi \frac{f_0}{f_s} n + \frac{\pi}{2} + \varphi_0 + \varphi_f\right) \\ &= mA_f \sin\left(2\pi \beta n + \frac{\pi}{2} + \varphi_0 + \varphi_f\right) \end{aligned} \quad (15)$$

Obviously, when $\beta \leq 0.5$, the sampling rate of the converter satisfies the Nyquist sampling theorem, and the output of the signal can be restored without deformation [15]. However, when $\beta > 0.5$, the sampling rate no longer satisfies the Nyquist sampling theorem, and the input signal frequency f_0 cannot be restored. Assume that

$$\beta = \text{floor}(\beta) + b = a + b \quad (16)$$

where $a = \text{floor}(\beta)$ is the integer part of α and b is the difference of β and a . By introducing (16) into (15), the sampling points of the converter can be written as

$$\begin{aligned} y_f[n] &= mA_f \sin\left(2\pi(a+b)n + \frac{\pi}{2} + \varphi_0 + \varphi_f\right) \\ &= mA_f \sin\left(2\pi bn + \frac{\pi}{2} + \varphi_0 + \varphi_f\right) \\ &= mA_f \sin\left(2\pi \frac{bf_s}{f_s} n + \frac{\pi}{2} + \varphi_0 + \varphi_f\right) \end{aligned} \quad (17)$$

From (17), it can be seen that only bf_s can be restored from the output signal. According to the Nyquist sampling theorem, the frequency of the output signal is less than the half of the sampling rate. Therefore, when $b \leq 0.5$, the output frequency is bf_s ; when $0.5 < b < 1$, (17) is written as follows:

$$\begin{aligned} y_f[n] &= mA_f \sin\left(2\pi \frac{bf_s}{f_s} n + \frac{\pi}{2} + \varphi_0 + \varphi_f\right) \\ &= mA_f \sin\left(2\pi \frac{(b-1)f_s}{f_s} n + \frac{\pi}{2} + \varphi_0 + \varphi_f\right) \\ &= mA_f \sin\left(2\pi \frac{(1-b)f_s}{f_s} n + \frac{\pi}{2} - \varphi_0 - \varphi_f\right) \end{aligned} \quad (18)$$

It is obvious that when $0.5 < b < 1$, the frequency of the output signal is $(1-b)f_s$, and the phase of the input signal will be changed from $(\pi/2) + \varphi_0 + \varphi_f$ into $(\pi/2) - \varphi_0 - \varphi_f$, resulting in the output waveform deformation of the Rogowski coil with the digital integrator.

3 Experiment results and analyses

In order to show the output waveform deformation phenomenon of the Rogowski coil current transformer with the digital integrator, an experiment is devised and the principle is shown in Fig. 6. Due to the limitations of the test conditions, the output of the Rogowski coil current transformer with the integrator is compared with that of the low LPCT, whose analogue output reflects the primary current input with no deformation and the transforming characteristics are basically the same with the electromagnetic transformer. The primary input current is sensed by both the LPCT and the Rogowski coil head. For the LPCT, the analogue output of the transformer is converted into the digital signal after passing the A/D converter. For the Rogowski coil, the analogue output of the head is first filtered and then converted by the A/D converter. Both the LPCT and the Rogowski coil current transformer share the same A/D converter on the sampling printed circuit board, and both the digital outputs of the converter are sent to the merging unit, and then the wave recording device to make a comparison.

To simplify the results, the outputs of the LPCT and Rogowski coil current transformer are called as 'Reference' and 'Digital integrating', respectively. Three kinds of input signals are used as shown in Table 1, and the sampling rate of the A/D converter is shown in Fig. 6, which is 4000 Hz as. The results of each input signal is recorded and shown in Figs. 7–9, respectively.

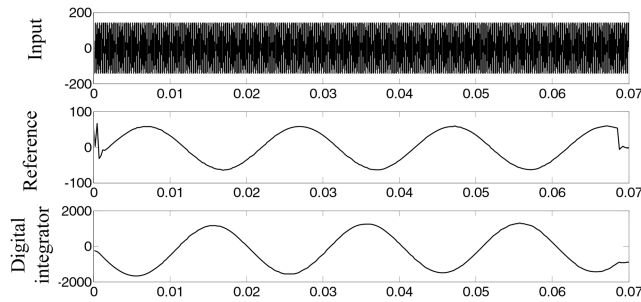


Fig. 8 Results of the 3950 Hz input signal

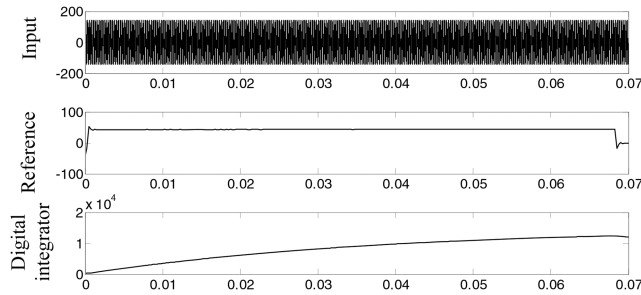


Fig. 9 Results of the 4000 Hz input signal

As shown in Fig. 7, the input signal is the power frequency signal with the amplitude of 100 A. Since the sampling rate of the A/D converter is 4000 Hz, which is far greater than the power frequency, the output of both LPCT and that of the Rogowski coil current transformer can restore the primary input current, and the results of 'Reference' and 'Digital integrator' are the same with the input. There is no frequency aliasing in such occasion.

When the frequency of the input signal is 3950 Hz, which is close to the sampling rate of the A/D converter, the Nyquist sampling theorem is not satisfied, and the output of 'Reference' and 'Digital integrator' are shown in Fig. 8. It can be seen that according to (14), the relationship between the input signal frequency and sampling frequency is $f_0 = 3950 \text{ Hz} = 0.9875 f_s$, which indicates that $\beta = b = 0.9875$. In Fig. 8, the output frequency of both 'Reference' and 'Digital integrator' are 50 Hz, which is exactly the same with $(1 - b)f_s$, and the initial phase of the 'Digital integrator' has transformed from 0 to π . The results of the output coincide well with the conclusion of (18).

As the input frequency grows to 4000 Hz, which is the same with the sampling rate, the LPCT always samples the same point in each cycle of the input signal and the output of the 'Reference' is a straight line. For the Rogowski coil current transformer, due to the integrating link of differential operation, as shown in Fig. 5, the output of the 'Digital integrator' keeps growing until it reaches the saturation point of the converter as shown in Fig. 9. Basically, the experimental results are in well agreements with the theoretical.

4 Methods to improve waveform deformation

In order to improve the waveform deformation and restore the input signal of the Rogowski coil current transformer with the digital integrator, several measures can be taken as follows:

- Increase the sampling rate of the converter. By increasing the sampling rate, the frequency aliasing threshold can be promoted, which will improve the output waveform deformation. However, this is not usually used in power systems because the sampling rate is usually stationary for the A/D sampling link.
- Decrease the cut-off frequency of the filter. As shown in Fig. 5, the cut-off frequency of the filter is one key factor to allow the wanted frequency signal. If the cut-off frequency is low, the unwanted high frequency generated by the system fault can be attenuated to a certain degree and then sent to the A/D converter, the frequency aliasing caused by the sampling link

will be alleviated. This method is only useful for the slowdown of the output waveform deformation, but cannot eliminate it thoroughly.

- Replace the digital integrator with the analogue integrator. From Figs. 4 and 5, it can be seen that for the Rogowski coil current transformer using the analogue integrator, the integrating link is right behind the differential operation. Therefore, the output signal of the Rogowski coil head can be immediately restored to the original wave before sampled by the converter, which avoids the frequency aliasing effectively. It is the most common method in the engineering application to prevent waveform deformation in the high-frequency current measurement of the Rogowski coil current transformer.

5 Conclusion

In this paper, the reason of the frequency aliasing phenomenon of the Rogowski coil transformer with the digital integrator is investigated by both theoretical analysis and experiment verification. Compared with the analogue integrator. Two parts of the output signal are influenced: magnitude enlarging and phase deviating. The integrating link is one key factor of the frequency aliasing, and the experiment is carried out to show the phenomenon vividly. Three methods to improve the waveform deformation are proposed and compared, and put the integrating link ahead before the sampling link is recommended to eliminate the frequency aliasing. The research is of great significance for the application of the Rogowski coil current transformer.

6 Acknowledgements

The author wishes to thank the IET for providing this template and all colleagues who previously provided technical support and advices. This paper is supported by Foundation of SGCC (No. JBB1720170082, Study on the Influences of VFOT on Outdoor Installation Protection Device and Its Testing Technologies).

7 References

- Mirko, M., Bernardo, T., Carmine, Z., *et al.*: 'Critical parameters for mutual inductance between Rogowski coil and primary conductor', *IEEE Trans. Instrum. Meas.*, 2011, **60**, (2), pp. 625–632
- Hemmati, E., Shahrtash, S.: 'Investigation on Rogowski coil performance for structuring its design methodology', *IET Sci. Meas. Technol.*, 2013, **7**, (6), pp. 306–314
- Mohammad, S., Arash, M., Mohammad, F.: 'The Rogowski coil principles and applications: A review', *IEEE Sens. J.*, 2015, **15**, (2), pp. 651–658
- Djokic, B.: 'Traceable calibrations of Rogowski coils at high AC currents', *IEEE Instrum. Meas. Mag.*, 2015, **18**, (6), pp. 12–17
- Qiang, G., Haow, L., Xiaomeng, X., *et al.*: 'A steady-state calibration method of electronic transformer based on improved digital filter algorithm', *Electr. Power Eng. Technol.*, 2018, **37**, (2), pp. 55–60
- Dubickas, V., Edin, H.: 'High-frequency model of the Rogowski coil with a small number of turns', *IEEE Trans. Instrum. Meas.*, 2007, **56**, (6), pp. 2284–2288
- Hanmiao, C., Qing, X., Feng, J.: 'A digital phase-shift method for phase compensation of electronic instrument transformers', *Electr. Power Eng. Technol.*, 2017, **36**, (2), pp. 82–87
- Qing, C., Hongbin, L., Mingming, Z., *et al.*: 'Design and characteristics of two Rogowski coils based on printed circuit board', *IEEE Trans. Instrum. and Meas.*, 2006, **55**, (3), pp. 939–943
- Tomoki, K., Shunichi, Y., Hiroaki, T., *et al.*: 'Development of a shunt lightning current measuring system using a Rogowski coil', *Electr. Power Syst. Res.*, 2015, **118**, pp. 110–113
- Ibrahim, A., Nassisi, V., Luches, A.: 'Coaxial-Cable wound Rogowski coils for measuring large-magnitude short-duration current pulses', *IEEE Trans. Instrum. Meas.*, 2013, **62**, (1), pp. 119–128
- Muhammad, S., Amjad, G., Lauri, K., *et al.*: 'Effect of geometrical parameters on high frequency performance of Rogowski coil for partial discharge measurements', *Measurement*, 2014, **49**, pp. 126–137
- Ibrahim, A.: 'Performance improvement of slow-wave Rogowski coil for high impulse current measurement', *IEEE Sens. J.*, 2013, **13**, (2), pp. 538–547
- Zuoqin, Z., Lixin, Z., Jinshan, C.: 'Study on structure parameters selection of Rogowski coil based on electromagnetic induction ability', *Electr. Meas. Instrum.*, 2014, **51**, (24), pp. 61–65
- Weibo, L., Chengxiong, M., Jiming, L.: 'Study of the virtual instrumentation applied to measure pulsed heavy currents', *IEEE Trans. Instrum. Meas.*, 2005, **54**, (1), pp. 284–288
- Rybin, Y., Petlina, T.: 'Basic metrological properties of electronic oscillators with direct digital synthesis', *Measurement*, 2017, **98**, pp. 243–249